Supporting Information

Non-Enzymatic Electrochemical Glucose Sensing by Cu_2O Octahedrons: Elucidating Protein Adsorption Signature

Soumyadipta Rakshit,[a] Srabanti Ghosh,[b] Rimi Roy[c] and Subhash Chandra Bhattacharya[a]*

[a] Department of Chemistry, Jadavpur University, Kolkata 700 032, India

[b] Department of Chemical, Biological and Macromolecular Sciences, S. N. Bose National Centre for Basic Sciences, Block JD, Sector III, Salt Lake, Kolkata 700 098, India.

[c] Department of Chemistry, Presidency University, Kolkata 700 073, India.

*E-mail: sbjuchem@yahoo.com; scbhattacharyya@chemistry.jdvu.ac.in

Tel: 033 2414 6223; Fax: (+) 91(033) 2414 6584

Contents

Fig. S1	FESEM, TEM and HRTEM images of Cu_2O microstructures along with schematic representation of growth mechanism.	S-2
Table ST1	Comparative study between the fabricated non-enzymatic glucose sensor and other literature works with respect to their performances.	S-3
Fig. S2	Amperometric response curve of the octahedron Cu_2O modified electrode derived from Figure 4a presenting the response time for the successive addition of glucose.	S-4
Fig. S3	Change in the amperometric current response of Cu_2O octahedron modified electrode towards successive addition of glucose.	S-4
Fig. S4	The plot of peak current difference as a function of the concentration of glucose.	S-5
Fig. S5	Amperometric response of the Cu_2O octahedron modified electrode in 0.1 M NaOH successive addition of human serum.	S-6
Fig. S6	Calibration Curve for different proteins in PBS buffer (pH~ 7.4) with experimentally determined data.	S-7
Fig. S7	The CD spectral changes of proteins in the absence and presence of Cu_2O octahedrons.	S-8
Fig. S8	Dynamic Light Scattering (DLS) graphs of native proteins and unadsorbed proteins in the supernatant.	S-9
Fig. S9	Dynamic Light Scattering graphs of Cu_2O octahedrons in the presence of proteins.	S-9
Table ST2	The estimated secondary structure content of proteins in the absence and presence of Cu_2O octahedrons.	S-10
Fig. S10	FESEM images of Cu_2O upon adsorption of different proteins.	S-11

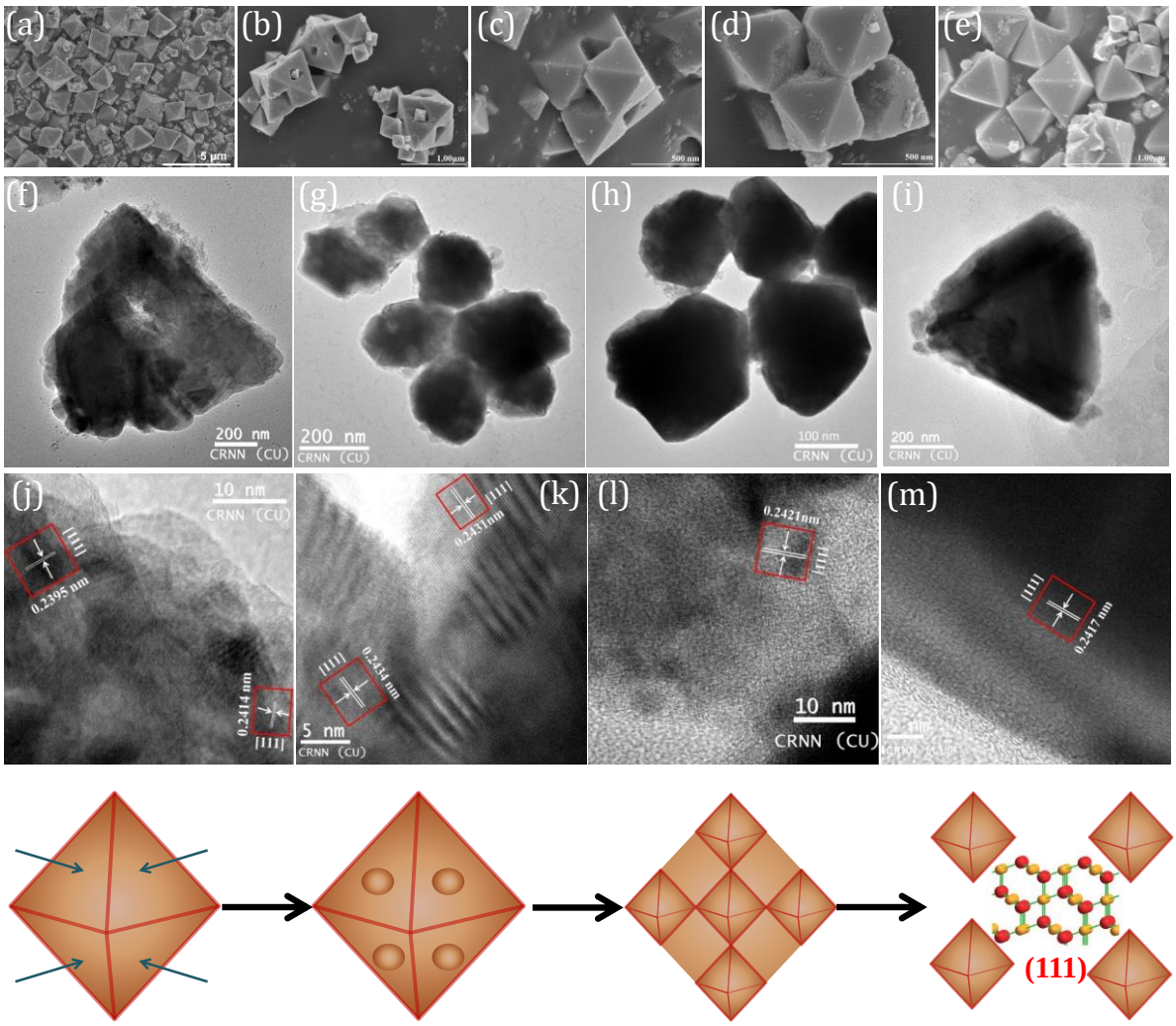

Fig. S1. (a), (b), (c), (d) and (e) are the FESEM images of Cu_2O microstructures fabricated at reaction times 10, 15, 20, 25 and 30 min. (f), (g), (h) and (i) illustrate the TEM images of Cu_2O octahedrons fabricated at reaction times 10, 15, 25 and 30 min. (j), (k), (l) and (m) represent corresponding HRTEM images. The lower panel displays a schematic representation of generation and growth mechanism of Cu_2O octahedrons along with the side views of (111) surfaces (Orange and red spheres indicate Cu and O atoms, respectively).

Table ST1. Comparative study between the fabricated non-enzymatic glucose sensor and other literature works with respect to their performances.

Type of electrode	Electrolyte	Response time (s)	Potential (V)	Sensitivity ($\mu A\ mM^{-1}\ cm^{-2}$)	Linear range (mM)	LOD (μM)	References
Porous Cu_2O	0.1 M NaOH	−	0.60	10.95	0.002–0.35	1.3	1
Hierarchical Cu_2O	0.1 M NaOH	−	0.60	13.3	0.05–1.1	47.2	2
Mesocrystalline Cu_2O hollow nanocubes	0.1 M NaOH	−	0.60	52.5	−	−	3
Helical TiO_2 nanotube arrays modified by Cu_2O	0.1 M NaOH	3	0.65	14.56	3.0−9.0	62.0	4
Cu_2O cubes/nafion	0.1 M NaOH	<5	0.60	121.7	−	38.0	5
Cubic Cu_2O	0.1 M NaOH	−	0.60	22.669	0.1–2.5	12.8	6
Cu_2O nanourchin with highly anisotropic nanoarms	0.1 M NaOH		0.60	1231.7	0.019–1.09	18.5	7
Cu/Cu_2O nanoclusters deposited carbon spheres	0.1 M NaOH	−	0.65	63.8	0.01–0.69	5.0	8
				22.6	1.19–3.69		
Copper oxide microspheres	0.1 M NaOH	<5	0.60	26.59	2.0–9.0	20.6	9
Spherical $Cu/CuO/SiO_2$ nanostructures	0.1 M NaOH	1	[-1 − +1]	8.0	3.0–12.0	1450	10
Cu_2O octahedrons	0.1 M NaOH	1.45	0.60	382.98	0.001−1.0	0.96	**This work**
				55.59	1.0–5.0		

References:

(1) L. Zhang, Y. H. Ni and H. Li, *Microchim. Acta*, 2010, **171**, 103–108.

(2) S. Li, Y. J. Zheng, G. W. W. Qin, Y. P. Ren, W. L. Pei and L. Zuo, *Talanta*, 2011, **85**, 1260–1264.

(3) Z. Gao, J. Liu, J. Chang, D. Wu, J. He, K. Wang, F. Xu and K. Jiang, *CrystEngComm*, 2012, **14**, 6639–6646.

(4) M. Long, L. Tan, H. Liu, Z. He, A. Tang, *Biosensors and Bioelectronics*, 2014, **59**, 243–250.

(5) S. Felix, P. Kollu, B.P.C. Raghupathy, S.K. Jeong, A.N. Nirmala Grace, *J. Chem. Sci.*, 2014, **126**, 25–32.

(6) L. Tang, J. Lv, C. Kong, Z. Yanga and J. Li., *New J. Chem.*, 2016, **40**, 6573–6576.

(7) J. He, Y. Jiang, J. Peng, C. Li, B. Yan, and X. Wang, *J Mater Sci*, 2016, **51**, 9696–9704.

(8) H. Yin, Z. Cui, L. Wang and Q. Nie, *Sensors and Actuators B* 2016, **222**, 1018–1023.

(9) M. Saraf, K. Natarajan and S. M. Mobin, *Dalton Trans.*, 2016, **45**, 5833–5840.

(10) N. Taşaltın, C. Taşaltın, S. Karakuş, A. Kilislioğlu, *Inorganic Chemistry Communications* 2020, **118**, 10799, 1–6.

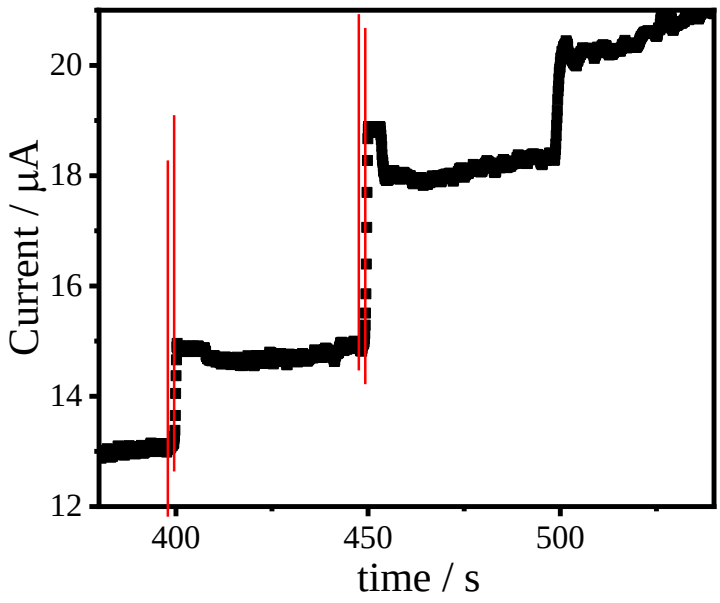

Fig. S2. Amperometric response curve of the octahedron Cu_2O modified electrode derived from Figure 4a presenting the response time for the successive addition of glucose.

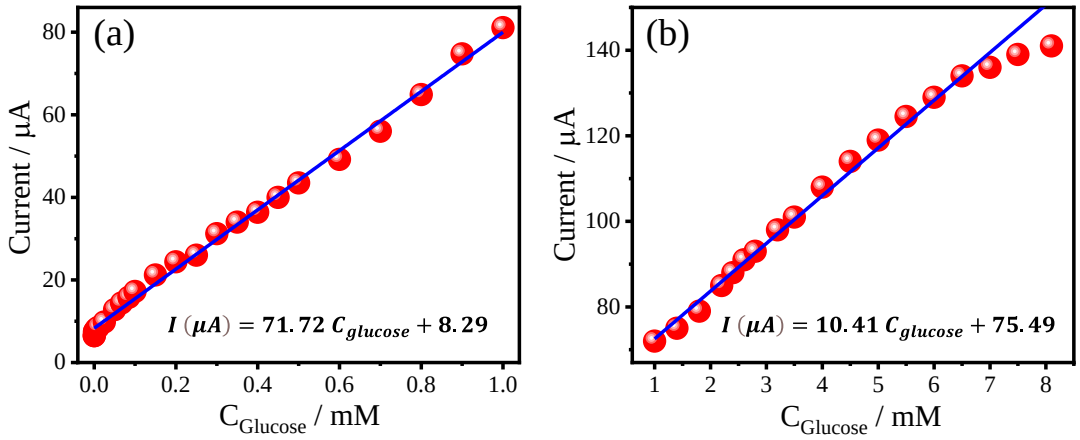

Fig. S3. Change in the amperometric current response of Cu_2O octahedron modified electrode towards successive addition of glucose. (a) depicts the linear range in the lower concentration range (0.1µM–1mM) and (b) demonstrates the higher concentration range (1–7 µM).

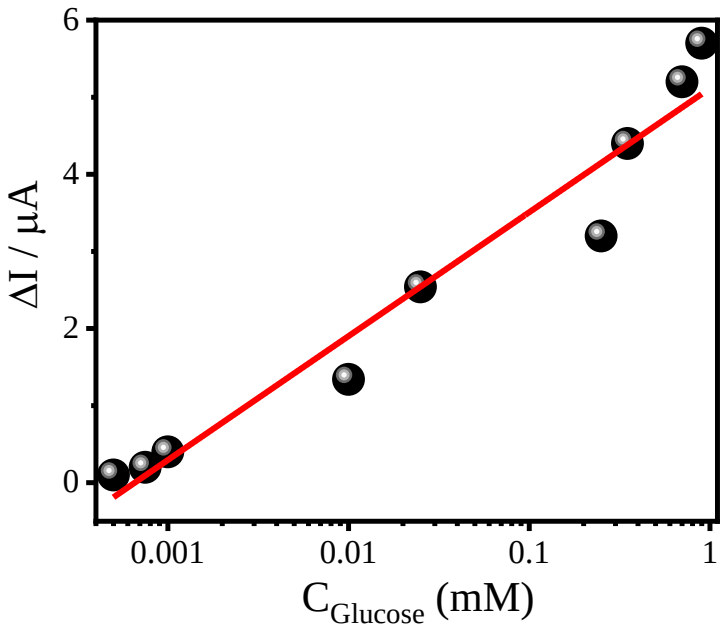

Fig. S4. The plot of peak current difference as a function of the concentration of glucose.

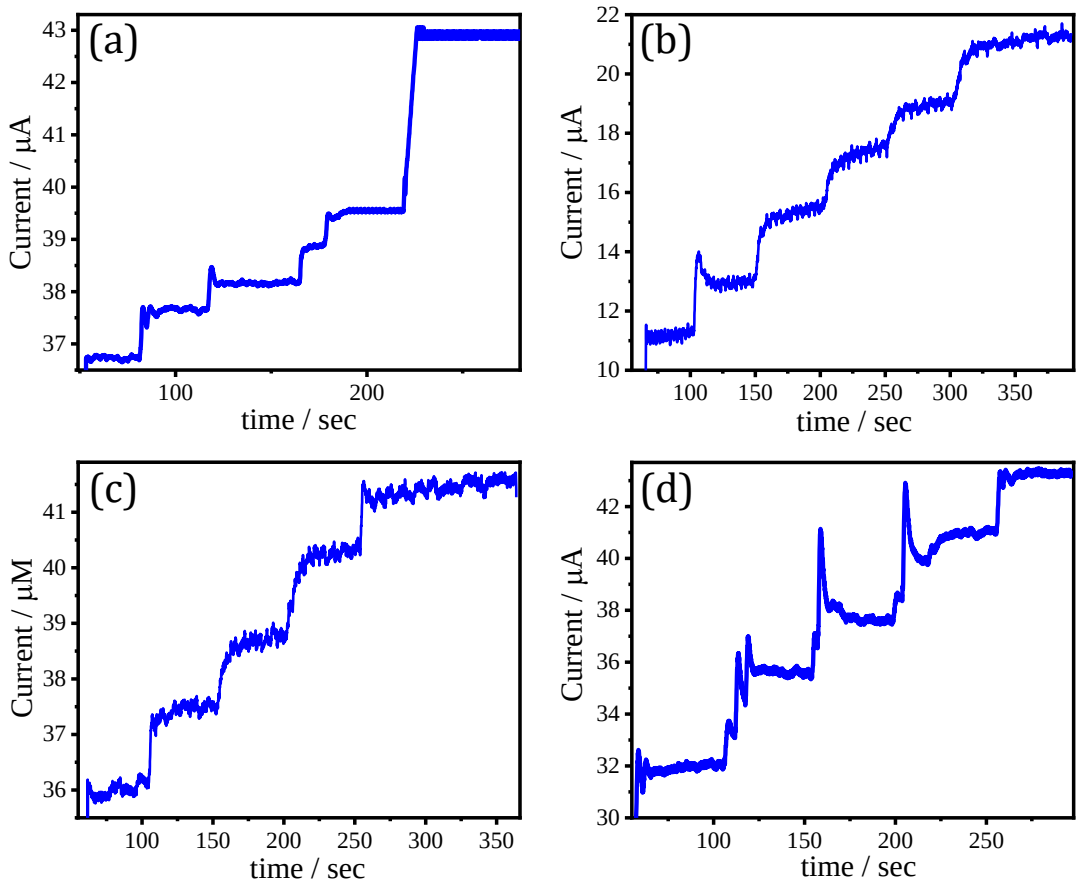

Fig. S5. Amperometric response of the Cu_2O octahedron modified electrode in 0.1 M NaOH under constant stirring with successive addition of human serum.

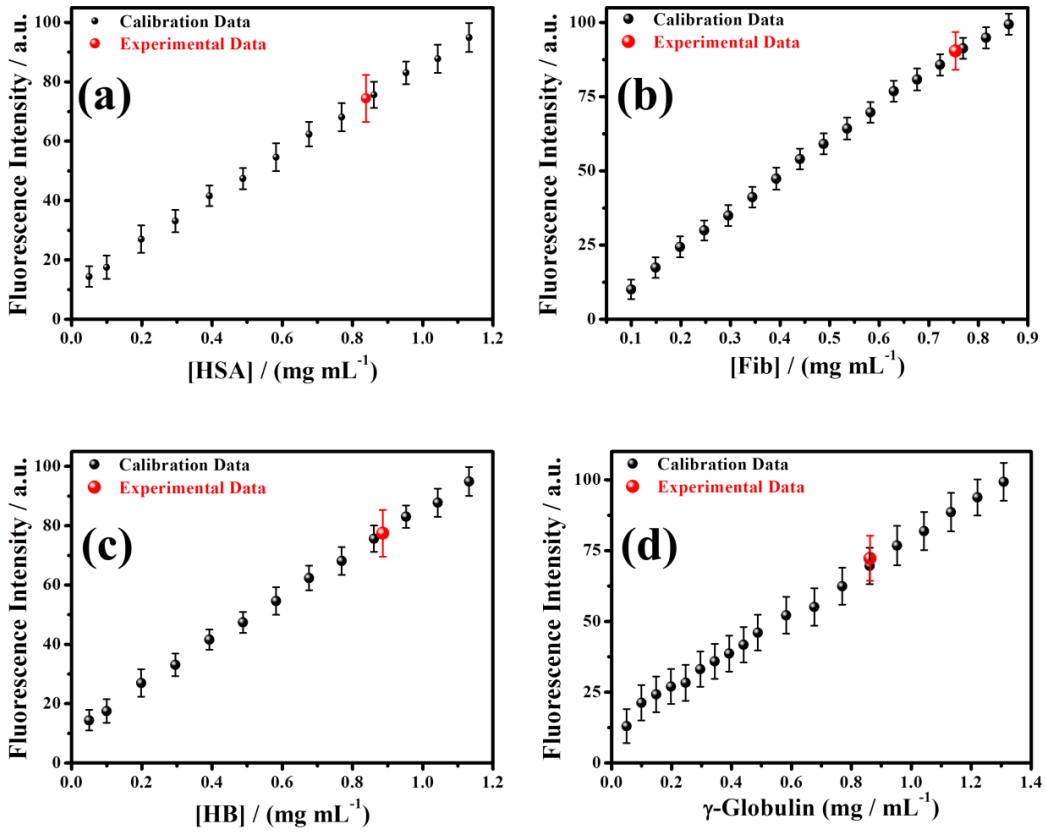

Fig. S6. Calibration Curve for different proteins (a) HSA, (b) Fibrinogen, (c) Hemoglobin, (d) γ-Globulin in PBS buffer (pH~ 7.4) with experimentally determined data.

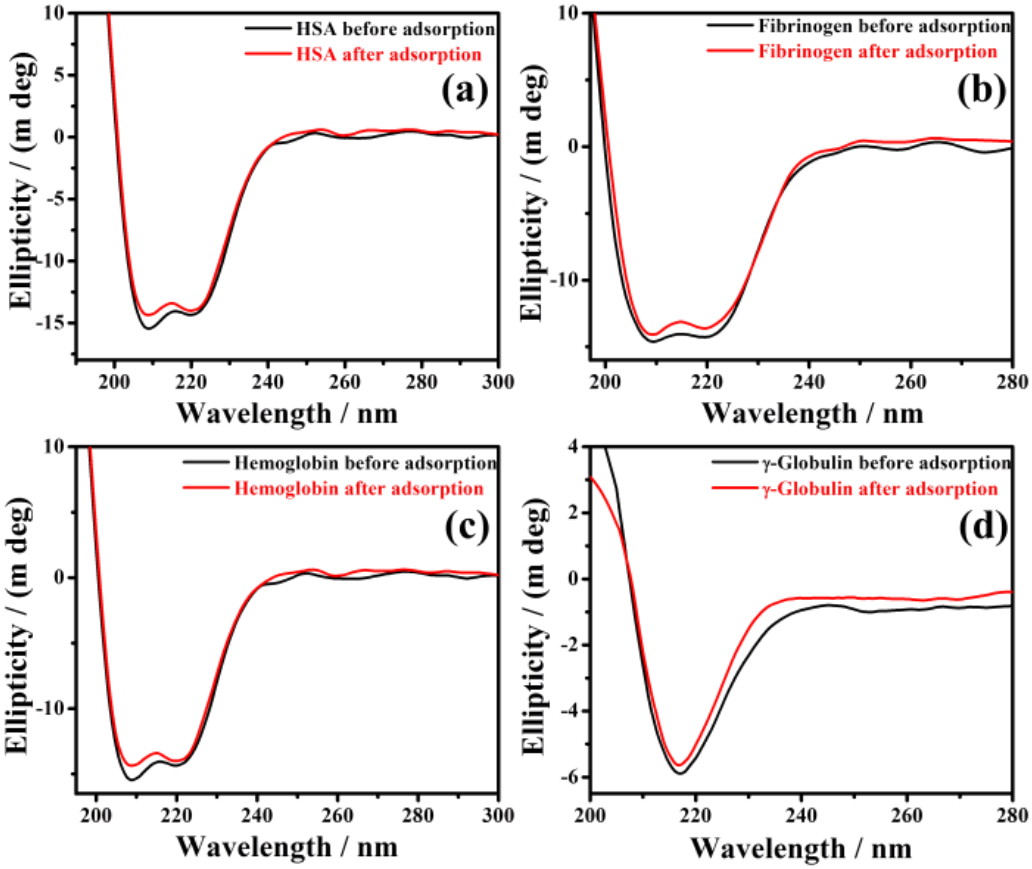

Fig. S7. The CD spectral changes of (a) HSA, (b) Fibrinogen, (c) Hemoglobin, (d) γ-Globulin in the absence and presence of Cu_2O octahedrons.

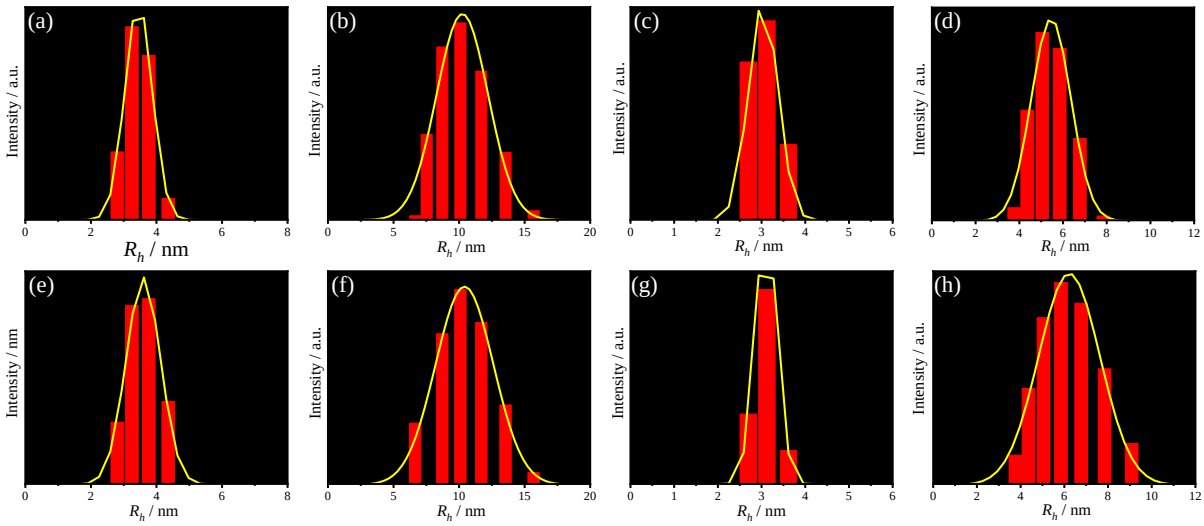

Fig. S8. Dynamic Light Scattering (DLS) graphs of native proteins (top row) and unadsorbed proteins in the supernant (bottom row); (a) & (e) HSA, (b) & (f) Fibrinogen, (c) & (g) Hemoglobin, (d) & (h) γ-Globulin.

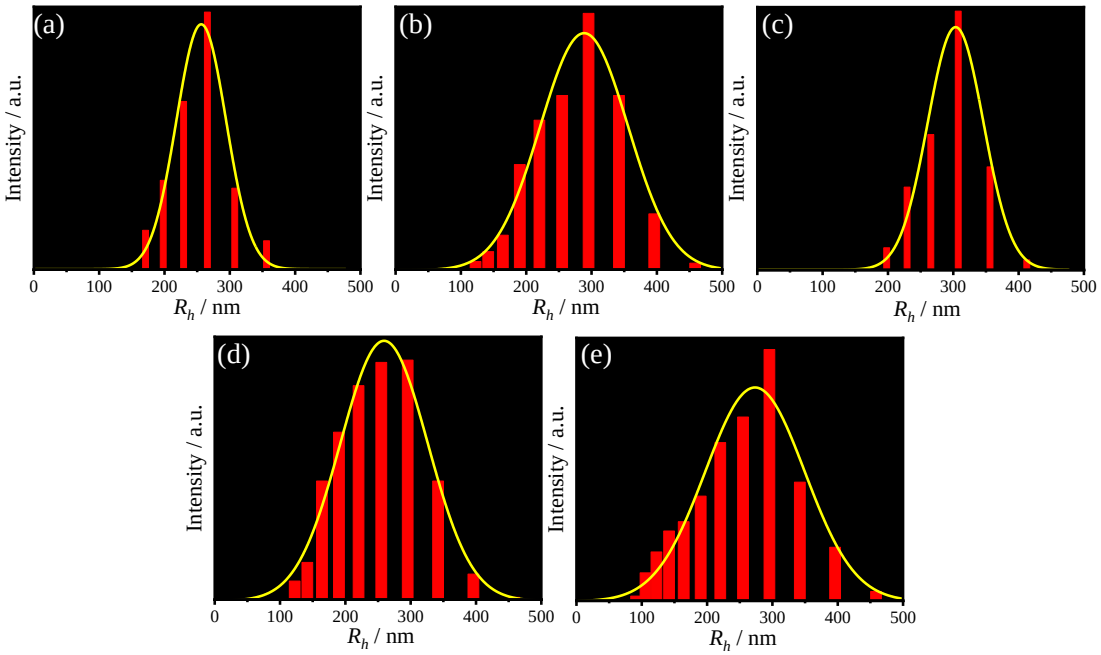

Fig. S9. Dynamic Light Scattering (DLS) graphs of (a) Cu_2O and in the presence of proteins (b) HSA, (c) Fibrinogen, (d) Hemoglobin, (e) γ-Globulin.

Table ST2. The estimated secondary structure content of proteins in the absence and presence of Cu_2O octahedrons.

System	CD				
	α-helix	***Antiparallel***	***Parallel***	***β-turn***	***Random***
Native HSA	67.60	2.90	3.00	12.10	13.00
HSA_Cu_2O	67.20	3.00	3.00	12.20	13.00
Native Fib	35.60	8.10	7.80	16.60	29.10
Fib_Cu_2O	34.90	8.20	8.10	16.70	30.10
Native Hb	66.70	2.90	3.40	11.90	15.60
Hb_Cu_2O	63.70	3.20	3.80	12.30	17.20
Native γ-GB	70.1	2.10	3.90	10.40	22.10
γ-GB_Cu_2O	67.3	2.30	4.10	10.80	22.80

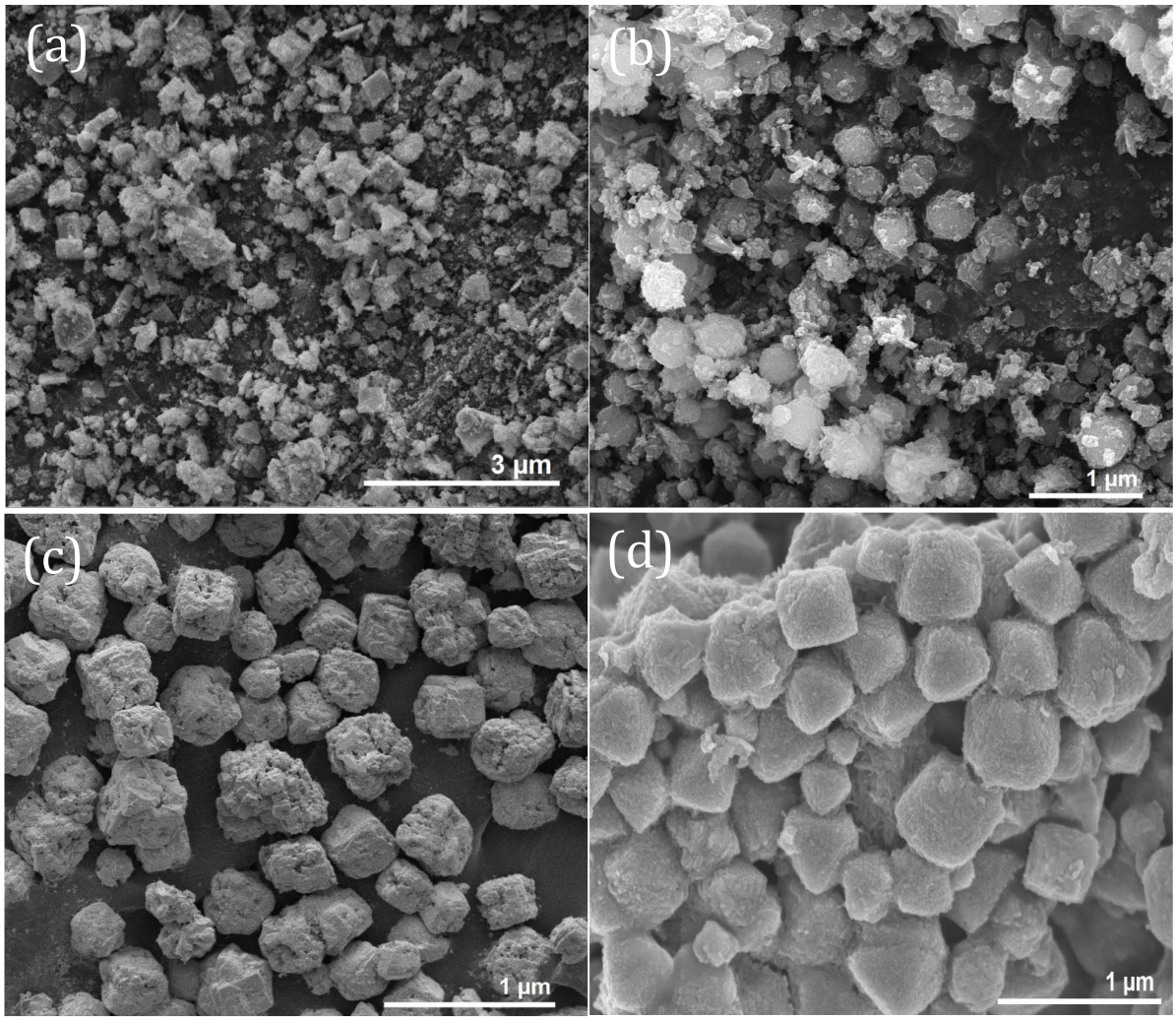

Fig. S10. FESEM images of Cu_2O microstructures upon adsorbing (a) Fibrinogen, (b) HSA, (c) γ-Globulin and (d) Hemoglobin.